

Title	Fast recovery of elastic constant in thin films studied by resonant-ultrasound spectroscopy
Author(s)	Nakamura, N.; Nakashima, T.; Ogi, H. et al.
Citation	Journal of Applied Physics. 2010, 107(10), p. 103541-1-103541-4
Version Type	VoR
URL	https://hdl.handle.net/11094/84227
rights	This article may be downloaded for personal use only. Any other use requires prior permission of the author and AIP Publishing. This article appeared in Journal of Applied Physics, 107(10), 103541 (2007) and may be found at https://doi.org/10.1063/1.3407540 .
Note	

Osaka University Knowledge Archive : OUKA

<https://ir.library.osaka-u.ac.jp/>

Osaka University

Fast recovery of elastic constant in thin films studied by resonant-ultrasound spectroscopy

Cite as: J. Appl. Phys. **107**, 103541 (2010); <https://doi.org/10.1063/1.3407540>

Submitted: 29 January 2010 . Accepted: 25 March 2010 . Published Online: 27 May 2010

N. Nakamura, T. Nakashima, H. Ogi, M. Hirao, and M. Nishiyama



View Online



Export Citation

ARTICLES YOU MAY BE INTERESTED IN

[Elastic stiffness of \$L1_0\$ FePt thin film studied by picosecond ultrasonics](#)

Applied Physics Letters **98**, 101911 (2011); <https://doi.org/10.1063/1.3562031>

[Nonlinear resonant ultrasound spectroscopy \(NRUS\) applied to damage assessment in bone](#)

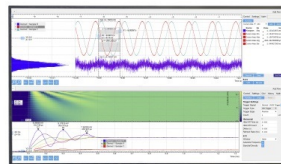
The Journal of the Acoustical Society of America **118**, 3946 (2005); <https://doi.org/10.1121/1.2126917>

[Determination of anisotropic elastic constants of superlattice thin films by resonant-ultrasound spectroscopy](#)

Journal of Applied Physics **97**, 013532 (2005); <https://doi.org/10.1063/1.1828221>

Challenge us.

What are your needs for
periodic signal detection?



Zurich
Instruments

Fast recovery of elastic constant in thin films studied by resonant-ultrasound spectroscopy

N. Nakamura,^{1,a)} T. Nakashima,¹ H. Ogi,¹ M. Hirao,¹ and M. Nishiyama²

¹Graduate School of Engineering Science, Osaka University, 1-3 Machikaneyama, Toyonaka, Osaka 560-8531, Japan

²Renovation Center of Instruments for Science Education and Technology, Osaka University, 1-2 Machikaneyama, Toyonaka, Osaka 560-0043, Japan

(Received 29 January 2010; accepted 25 March 2010; published online 27 May 2010)

This paper reports incredibly large and rapid evolution of elastic constants in deposited copper and silver films observed by the resonant-ultrasound spectroscopy. The evolution begins just after stopping the deposition with the temperature dependent recovery rate. To explain the mechanism, we propose a model, where the elastic constants at grain boundary regions increase by 67% at least. Diffusion of atoms along the grain boundary region is a possible reason, and we confirm that the activation energy is much smaller than that for grain-boundary diffusion in bulk materials. These results are explained by drastic structure change at grain boundaries, being similar to phase transition from liquid into solid phase. © 2010 American Institute of Physics. [doi:10.1063/1.3407540]

I. INTRODUCTION

Recovery and recrystallization usually occur when a solid is heated or deformed. However, in polycrystalline thin films, they occur after stopping deposition without being heated or deformed.¹⁻³ It has been considered that atoms at film surface and grain boundaries are thermodynamically unstable during and just after the deposition, and recovery and recrystallization occur to make the film thermodynamically stable by causing atoms to flow between the film surface and grain boundary. Among studies on recovery, curvature measurements found a drastic stress evolution that in-plane intrinsic stress changes from compressive to tensile just after stopping the deposition.⁴⁻⁹ Considering that sign of the stress is changed and a large part of the stress evolution completes within several tens of minutes, fast and drastic structure evolution is thought to occur in the films. Especially, as indicated, recovery is associated with the structure change at the grain boundaries. Chason *et al.*,¹⁰ for example, observed the recovery of the in-plane stress in Ag polycrystalline thin films and they attributed this to the diffusion of excess atoms from grain boundary regions to surface. Finite element method¹¹ and molecular dynamics simulation¹² also expect that the structure evolution at grain boundaries contributes to the stress evolution. X-ray diffraction analysis,¹ cross-sectional observation using focused ion beam,² and *in situ* real-time reflection high-energy electron diffraction¹³ are used for studying the structure evolution in thin films. However, they cannot monitor the rapid structure evolution and are not sensitive to the local structure change. Scanning tunneling microscopy has contributed to understand the structure evolution at the surface,¹⁴⁻¹⁶ and *in situ* measurement is possible.¹⁷ However, observable region is limited to the surface, and in continuous films it cannot necessarily observe the diffusion at grain boundary. Therefore, there is still con-

siderable controversy over the structure evolution at grain boundary; to understand the recovery phenomena, we need a novel measurement, which is sensitive to the grain-boundary structures.

We then focus on the elastic constants. They inherently reflect the interatomic bond strength and decrease when thin incohesive bonds are included.^{18,19} Thus, monitoring the elastic constants during the recovery provides us with the essence of the recovery phenomena in thin films. It enables us to discuss the microstructural evolution at the grain boundaries inversely. In addition, this study has a significant effect on the curvature measurements. In curvature measurements, elastic constants of thin films are required in converting the curvature to the stress and eliminating the thermal stress from the measured stress. In the calculations, elastic constants have been considered to be comparable to those of the bulk materials. However, elastic constants actually show recovery as described later, and for quantitative evaluation of the stress recovery, the elastic recovery has to be considered. For these reasons, study on elastic recovery plays an important role for understanding the recovery, but measurement of the elastic constants of thin films is never straightforward; conventional methods were impossible to monitor the elastic recovery. This problem is solved by using an advanced resonant-ultrasound spectroscopy.²⁰ Elastic recovery of Cu and Ag films is investigated, and the results are compared with the previously reported stress-recovery behavior. Then, we propose a model to explain the elastic recovery.

II. EXPERIMENTS

Elastic recovery is monitored by measuring a free-vibration resonance frequency of a substrate on which film is deposited. Before deposition, the substrate's resonance frequency is measured, which depends on the mass density, dimensions, and elastic constants, C_{ij} .^{21,22} During deposition, the resonance frequency changes depending on the mass den-

^{a)}Electronic mail: nobutomo@me.es.osaka-u.ac.jp.

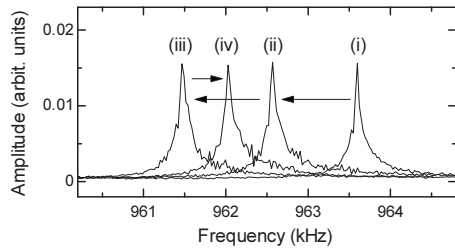


FIG. 1. Resonance spectra of the monocrystal Si substrate at (i) before, (ii) during, (iii) just stopping, and (iv) after stopping deposition of Cu film of the final thickness of 195 nm: (i), (ii), (iii), and (iv) denotes the time indicated by arrows in Fig. 2.

sity, thickness, and C_{ij} of deposited film. After stopping the deposition, mass density, dimensions, and C_{ij} of the substrate are unchanged, and the film thickness is also constant. Recovery could cure the nanoscale defects, and the mass density of the film may increase, which will decrease the resonance frequency. However, as shown later, resonance frequencies actually increase after stopping the deposition; the mass density increment cannot explain this observation. Therefore, the frequency evolution is attributed to the elastic recovery of the film.

Frequency evolution is monitored using tripod needle transducer. It consists of two piezoelectric pinducers and a needle-shape thermocouple, and is located in the sputtering chamber; a substrate is placed on the tripod transducer. A pinducer is driven by a sinusoidal continuous wave (cw) signal of typically 20 V_{pp} that is generated by the synthesizer. The pinducer vibrates the substrate. The other pinducer detects the vibrational amplitude of the substrate. By changing the frequency of the cw signal, a resonance spectrum is obtained. This involves no coupling agent and no external force except for the own weight of the substrate, realizing an ideal free-vibrations measurement. The tripod needle transducer is connected to a heat exchanger vessel. By filling the vessel with the liquid nitrogen, the substrate is cooled down to about -44 °C. Detail of the measurement setup is shown in the supplemental file²³ and elsewhere.²⁰

Cu or Ag is deposited on rectangular-parallelepiped substrates of monocrystal Si, typically measuring $3.500 \times 3.000 \times 0.100$ mm³, by the rf-magnetron sputtering. Edges of the substrates are parallel to [100], [010], and [001] directions, respectively. Typical resonance spectrum of a Si substrate is shown in Fig. 1(i). When the frequency of cw signal corresponds to a resonance frequency of the substrate, the resonance spectrum shows a peak. Lorentz function is fitted around the peak, and the center frequency is defined as the resonance frequency. Before deposition, the background pressure was less than 4.0×10^{-4} Pa. During the deposition, Ar pressure was 0.4 Pa. Substrate temperature ranged from -44 °C to room temperature. Film thickness was determined by x-ray reflectivity measurements^{24,25} after deposition, and the typical film thicknesses were 200 nm and 250 nm for Cu and Ag films, respectively. X-ray diffraction measurements showed (111) texture for both of them in the thickness direction.

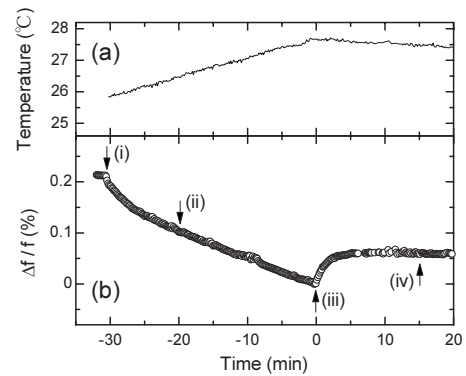


FIG. 2. (a) Substrate temperature and (b) change ratio of the resonance frequency of a Si substrate before, during, and after deposition of Cu film of 195 nm thickness: Cu was deposited for 30 min and the deposition was stopped at $t=0$.

III. RESULTS

Figure 2 shows typical evolutions of the resonance frequency and the substrate temperature. Figure 1 shows the resonance spectra at four moments indicated by arrows in Fig. 2. Deposition was started at -30 min and was stopped at 0 min. Resonance frequency decreased from the beginning of deposition due to the mass loading, and rapidly increased after stopping the deposition. Increment ratio of the resonance frequency at room temperature was 0.023%–0.060% and 0.039%–0.087% for Cu and Ag film, respectively. The substrate temperature monotonically increased by about 2 °C during the deposition, and it slowly decreased afterward. Figure 3 shows the enlarged view of the increment behavior of the resonance frequency after stopping the deposition. The slower frequency increment appears at lower substrate temperature.

IV. DISCUSSION

There are two possible factors causing the frequency increments: (i) temperature dependence of C_{ij} and (ii) recovery of the thin film C_{ij} . Temperature decrement usually increases the elastic constants, and may consequently increase the resonance frequencies. The influence can be evaluated by calculating the resonance frequency of film/substrate layered specimen by Rayleigh–Ritz method²⁶ using the reported temperature dependence of C_{ij} .²⁷ In this calculation, we assume that thin films have the (111) texture; $\langle 111 \rangle$ direction of all

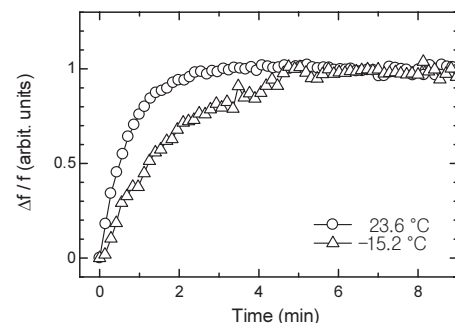


FIG. 3. Frequency evolutions after stopping deposition of Ag of 255 nm, open circles denote the evolution at room temperature, and open triangles the evolution at -15.2 °C.

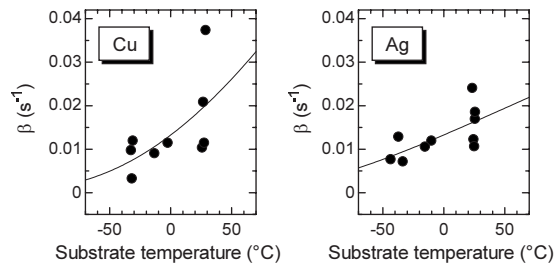


FIG. 4. Recovery rate, β , of elastic recoveries at several temperatures. Curves are fitted Arrhenius functions.

grains is perpendicular to the film surface and the grains are randomly oriented around the film-thickness direction. Then, the thin film shows transverse isotropy (hexagonal symmetry), and possesses five independent C_{ij} . They are calculated using the C_{ij} of single crystal Cu and Ag by Hill's averaging method.²⁸ In Fig. 2, the resonance frequency increases by 0.058% and the substrate temperature decreases by 0.8 °C through the cooling stage. Rayleigh–Ritz calculations indicated that this temperature change increases the resonance frequency of Cu/Si layered specimen by only 0.0009%, mainly from the substrate. This is much smaller than the observed frequency increment of 0.058%. Therefore, the temperature change cannot explain the observed frequency increment, and it is attributed to the recovery of thin film C_{ij} . Among the thin film C_{ij} , the in-plane longitudinal elastic constant, C_{11} , usually shows the largest contribution to the resonance frequencies of the film/substrate layered specimen,²⁹ which indicates that frequency evolution reflects mainly the recovery of C_{11} . Assuming that the resonance frequency depends solely on C_{11} , it was calculated that the frequency recovery in Fig. 2 corresponds to 15.2% increment of C_{11} . In bulk Al, the recovery is reported to increase the elastic constant by 0.12% after plastic deformation.³⁰ Comparing with this, the recovery degree of thin film's C_{11} is surprisingly larger.

Next, we consider the temperature dependence of the recovery speed. Chason *et al.*¹⁰ approximated the stress recovery by exponential function, $\sigma \propto \exp(-\beta t)$, and evaluated the recovery speed by deducing the relaxation rate, β ; β of the stress recovery was 0.0093 s⁻¹ for Ag films. We also assume that the elastic-constant recovery obeys the exponential law. Determined β , shown in Fig. 4, is almost the same as that of stress recovery, and decreases as the substrate temperature decreases. In Fig. 4, the temperature dependence of β is approximated by Arrhenius equation, $\beta = \beta_0 e^{-E_m/kT}$, and the activation energy of the elastic recovery, E_m , is deduced to be 0.103 eV and 0.058 eV in Cu and Ag films, respectively. k is Boltzmann constant and T the substrate temperature in unit of kelvin. β_0 is the relaxation rate at the high-temperature limit. In bulk Cu, activation energies for self diffusion and boundary diffusion are 2.04 eV and 1.08 eV, respectively,³¹ and in Cu films, activation energy for electromigration is 0.8–0.91 eV.^{32,33} Comparing with them, activation energy for the elastic recovery is significantly smaller, which indicates that the recovery speed is faster.

The above observations indicate that the elastic recovery progresses faster and the recovery degree is significantly

larger than in bulk materials. We here consider mechanism of the elastic recovery. In the case of the stress recovery, two kinds of models have been proposed. In one of them, Spaepen³⁴ and Friesen and Thompson³⁵ considered that the stress evolution is associated with atoms at and near ledges on the surface of the film. During film deposition, the film surface is not in equilibrium, and ledges exist on the surface. When deposition is stopped, the film smoothens, which decreases the compressive surface stress and causes a tensile increase. In the other model, Chason *et al.*¹⁰ explained the stress evolution by the flow of atoms at grain boundaries. This model assumes that during deposition the chemical potential of atoms on the film surface is higher than that at the grain boundaries, which drives excess atoms into the grain boundaries inducing a compressive stress in the film. When the deposition stops, the surface chemical potential rapidly decreases, and the atoms flow out of the grain boundary to the surface, causing tensile stress. In polycrystalline films, it has been demonstrated that the elastic constants are highly sensitive to the binding conditions at the grain boundaries.^{18,19} Therefore, we consider that the elastic recovery is explained by the structure evolution at the grain boundaries rather than the surface reconstruction and elastic constants at the grain boundary regions increase after stopping the deposition.

In the following discussion, we focus on the recovery degree at the grain boundary regions, which are simulated by penny-shape thin inclusions. We propose a polycrystalline film model, in which elastic constants at grain boundary regions, C'_{ij} , asymptotically increase with time,

$$C'_{ij}(t) = C_{ij}^0 [1 - A \exp(-t/\alpha)], \quad (1)$$

and the elastic constants within the grains are unchanged. Here, C_{ij}^0 are the elastic constants in the grains. α governs the recovery speed, and A determines the increment degree of the elastic constants. We assume that weak bonding regions at grain boundary have penny-shape with elastic constant C'_{ij} , and they are aligned parallel to the film-thickness direction in an isotropic matrix of polycrystalline Cu or Ag, which has the columnar microstructure. C_{ij} of this composite can be calculated using micromechanics modeling.¹⁸ The modeling takes two steps. First, we calculate the C_{ij} of a composite, in which minor axes of penny-shape inclusions of air are aligned in one direction parallel to the surface. Such a material macroscopically shows hexagonal symmetry and has five independent elastic constants. Second, we average the hexagonal symmetry elastic constants around the thickness direction, x_3 axis, by Hill's approximation. The resulting elastic constants, \bar{C}_{ij} , show transverse isotropy about the film-thickness direction. Detail of this modeling is described in the supplemental file.²³

Recovery degree, A , is evaluated by comparing the measured and calculated elastic recovery together with other unknown parameters: aspect ratio, volume fraction, and α of weak bonding regions. We calculated the elastic recovery by changing these parameters, and found that the aspect ratio hardly affects both recovery speed and recovery degree in the range between 0.0001 and 0.01. On the other hand, the recovery speed was closely related with α , and the recovery

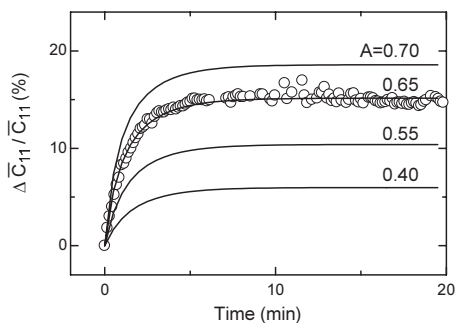


FIG. 5. Open circles denote the evolution of C_{11} after stopping the deposition of Cu film of 195 nm thickness. Curves denote the elastic recovery calculated by the proposed model with various A .

degree highly depended on the volume fraction and A . From these results, the volume fraction has to be determined to infer A . However, it is quite difficult to determine it by experiments. We here overestimate the volume fraction (10%) to estimate the minimum value of A . In Fig. 5, calculated elastic recovery behaviors are compared with the typical elastic recovery deduced from the measured frequency evolution. In this study, we observed that the recovery degree of C_{11} was larger than 7%. Figure 5 indicates that A has to be larger than 0.4 to reproduce the recovery degree, which indicates that the elastic constant at the grain boundary regions increases by at least 67% [$=A/(1-A)$].

We consider that this stiffening at the grain boundaries is explained by the local structure change from liquidlike structure (not amorphous) into solid structure. Temperature dependence of β supports this view. In bulk Cu, E_m of boundary diffusion is 1.08 eV. By assuming that E_m of boundary diffusion in Cu thin film is the same as that in the bulk Cu, temperature at the grain boundaries can be deduced from the Arrhenius equation. In this study, we observed that average β and β_0 are 0.013 s^{-1} and 1.064 s^{-1} , respectively. From these parameters, the apparent temperature at the grain boundaries, T , is estimated to be 2840 °C, which is larger than the melting point of bulk Cu (1084.5 °C). This result indicates that the elastic constants at the grain boundaries are much smaller than those of bulk Cu due to nearly liquid phase or supercooling phase, and the transition into the solid phase occurs within a few minutes after the deposition, which increases the elastic constants, causing the rapid and significant elastic recovery. Amorphous structure may be a possible factor which softens the grain boundaries. However, for example, elastic constants of amorphous structure is smaller than those of the corresponding crystal by 2%–36%,³⁶ and it cannot explain the observed increment. Therefore, drastic structure evolution like liquid-solid transition is a possible mechanism of the elastic recovery.

V. CONCLUSION

In summary, recovery of elastic constants of Cu and Ag films was observed after stopping deposition. To explain the recovery, we developed the model that elastic constants at

the grain boundaries recover by the solidification, leading to the increment of the macroscopic elastic constants. This model estimated that the elastic recovery at the grain boundaries exceeds 67%. In the common studies on stress evolution, intrinsic stress was deduced from the curvature change assuming that elastic constants of thin films are unchanged by the recovery. However, our finding indicates that this assumption is inappropriate and the elastic recovery has to be considered to quantitatively evaluate the stress recovery. This knowledge must play an important role in the future research on recovery.

- ¹J. W. Patten, E. D. McClanahan, and J. W. Johnston, *J. Appl. Phys.* **42**, 4371 (1971).
- ²C. Lingk and M. E. Gross, *J. Appl. Phys.* **84**, 5547 (1998).
- ³S. H. Brongersma, E. Richard, I. Vervoort, H. Bender, W. Vandervorst, S. Lagrange, G. Beyer, and K. Maex, *J. Appl. Phys.* **86**, 3642 (1999).
- ⁴R. Koch and R. Abermann, *Thin Solid Films* **140**, 217 (1986).
- ⁵D. Winau, R. Koch, A. Führmann, and K. H. Rieder, *J. Appl. Phys.* **70**, 3081 (1991).
- ⁶A. L. Shull and F. Spaepen, *J. Appl. Phys.* **80**, 6243 (1996).
- ⁷W. D. Nix and B. M. Clemens, *J. Mater. Res.* **14**, 3467 (1999).
- ⁸A. L. Del Vecchio and F. Spaepen, *J. Appl. Phys.* **101**, 063518 (2007).
- ⁹J. W. Shin and E. Chason, *Phys. Rev. Lett.* **103**, 056102 (2009).
- ¹⁰E. Chason, B. W. Sheldon, L. B. Freund, J. A. Floro, and S. J. Hearne, *Phys. Rev. Lett.* **88**, 156103 (2002).
- ¹¹J. S. Tello, A. F. Bower, E. Chason, and B. W. Sheldon, *Phys. Rev. Lett.* **98**, 216104 (2007).
- ¹²C. W. Pao, S. M. Foiles, E. B. Webb, D. J. Srolovitz, and J. A. Floro, *Phys. Rev. Lett.* **99**, 036102 (2007).
- ¹³C. Friesen and C. V. Thompson, *Phys. Rev. Lett.* **93**, 056104 (2004).
- ¹⁴M. Poensgen, J. F. Wolf, J. Frohn, M. Giesen, and H. Ibach, *Surf. Sci.* **274**, 430 (1992).
- ¹⁵W. W. Pai, N. C. Bartlett, and J. E. Reutt-Robey, *Phys. Rev. B* **53**, 15991 (1996).
- ¹⁶M. Giesen and G. S. Icking-Konert, *Surf. Sci.* **412–413**, 645 (1998).
- ¹⁷M. J. Rost, *Phys. Rev. Lett.* **99**, 266101 (2007).
- ¹⁸N. Nakamura, H. Ogi, and M. Hirao, *Acta Mater.* **52**, 765 (2004).
- ¹⁹H. Ogi, N. Nakamura, H. Tanei, R. Ikeda, M. Hirao, and M. Takemoto, *Appl. Phys. Lett.* **86**, 231904 (2005).
- ²⁰N. Nakamura, H. Ogi, T. Nakashima, M. Hirao, and M. Nishiyama, *Jpn. J. Appl. Phys., Part 1* **46**, 4450 (2007).
- ²¹I. Ohno, *J. Phys. Earth* **24**, 355 (1976).
- ²²A. Migliori, J. L. Sarrao, W. M. Visscher, T. M. Bell, M. Lei, Z. Fisk, and R. G. Leisure, *Physica B* **183**, 1 (1993).
- ²³See supplementary material at <http://dx.doi.org/10.1063/1.3407540> for details of the modeling and measurement setup.
- ²⁴H. Kiessig, *Ann. Phys.* **402**, 769 (1931).
- ²⁵L. G. Parratt, *Phys. Rev.* **95**, 359 (1954).
- ²⁶P. Heyliger, *J. Acoust. Soc. Am.* **107**, 1235 (2000).
- ²⁷G. Simmons and H. Wang, *Single Crystal Elastic Constants and Calculated Aggregate Properties: A Handbook* (MIT, Cambridge, 1971).
- ²⁸R. Hill, *J. Mech. Phys. Solids* **11**, 357 (1963).
- ²⁹N. Nakamura, H. Ogi, M. Hirao, and T. Ono, *J. Appl. Phys.* **97**, 013532 (2005).
- ³⁰H. Ogi, A. Tsujimoto, M. Hirao, and H. Ledbetter, *Acta Mater.* **47**, 3745 (1999).
- ³¹F. J. Humphreys and M. Hatherly, *Recrystallization and Related Annealing Phenomena* (Pergamon, Oxford, 1995).
- ³²K. D. Lee, E. T. Ogawa, S. Yoon, X. Lu, and P. S. Ho, *Appl. Phys. Lett.* **82**, 2032 (2003).
- ³³J. W. Pyun, W. C. Baek, L. Zhang, J. Im, P. S. Ho, L. Smith, and G. Smith, *J. Appl. Phys.* **102**, 093516 (2007).
- ³⁴F. Spaepen, *Acta Mater.* **48**, 31 (2000).
- ³⁵C. Friesen and C. V. Thompson, *Phys. Rev. Lett.* **89**, 126103 (2002).
- ³⁶D. J. Safarik and R. B. Schwarz, *Acta Mater.* **55**, 5736 (2007).